Desalination and Water Treatment
www.deswater.com

doi: 10.1080/19443994.2016.1167626

57 (2016) 27085–27095
December

Taylor & Francis
Taylor & Francis Group

Alternatives for vacuum generation in unconventional seawater desalination systems

Héctor Miguel Aviña Jiménez[a,*], Gabriel León de los Santos[b], Daniel Sauceda Carbajal[c], Fernando García Torres[a], Miguel Ángel Benítez Torreblanca[a]

[a]*Grupo iiDEA, Instituto de Ingeniería, Universidad Nacional Autónoma de México, Ciudad de México, Mexico, Tel. +52 55 5623 3500, ext. 1652; email: HAvinaJ@iingen.unam.mx (H.M. Aviña Jiménez), Tel. +52 55 5623 3500, ext. 1650; emails: GarciaFernando.T@gmail.com (F. García Torres), MBenitezT@iingen.unam.mx (M.Á. Benítez Torreblanca)*
[b]*División de Ingeniería Eléctrica, Facultad de Ingeniería, Universidad Nacional Autónoma de México, Ciudad de México, Mexico, Tel. +52 55 5622 3035; email: tesgleon@yahoo.com*
[c]*División de Física Aplicada, Departamento de Electrónica y Telecomunicaciones, Centro de Investigación Científica y de Educación Superior de Ensenada, Baja California, Mexico, Tel. +52 646 175 0500, ext. 25322; email: dsauceda@cicese.mx*

Received 15 October 2015; Accepted 15 March 2016

ABSTRACT

Seawater desalination is a viable option to reduce water shortage problems. As a consequence, the development of technologies that can guarantee the availability of water resources is essential. This article primarily focuses on the study and theoretical analysis of a vacuum generation system for a modular desalination unit with low-enthalpy geothermal energy as power source. This desalination unit, currently in the Research & Development stage, aims to be an effective, low-cost and marketable product, fulfilling the need of water in regions that have both, the energy source, and the lack of drinking water, such as northwestern Mexico. Based on the dissertation presented, the use of a hydroejector is proposed, discussing the feasibility of the use of steam or air as working fluid.

Keywords: Vacuum generation; Seawater desalination; Multiple-effect distillation; Low-enthalpy geothermal energy; Brackish water desalination

1. Introduction

Water is an essential, natural resource for life, however, its overexploitation has caused global shortage problems. On the other hand, desalination of seawater is a viable option to reduce local water shortage problems, for both consumption and use. Thus, the development of technologies promoting the availability of water resources is essential. The present work resides in this area, providing an alternative for vacuum generation in a geothermal desalination unit.

Discussing conventional technologies, vacuum inside evaporation chambers in systems that use thermal energy to evaporate seawater (MSF, MED, VCT, and SD) is essential as it allows the decrease in the saturation point of seawater, enabling an improved use of energy resources and increasing the production of distilled water. The extraction of non-condensable gases in the evaporation chambers is vital for the proper functioning of the plant since the accumulation of these gases affects the process of heat transfer to

*Corresponding author.

seawater, therefore, decreasing the overall performance of the plant.

Plants whose operating principle is based on seawater distillation are commonly installed near conventional power plants, where desalination plants can recover energy from steam turbines or waste heat sources and then use it to generate vacuum. Thus, the analysis of the vacuum equipment is also relevant.

Usually, the process of vacuum generation involves ejectors, using a primary fluid at high speed to drag a secondary fluid into a mixing chamber, generating vacuum in the secondary fluid reservoir. A general diagram of the device is shown in Fig. 1.

The working fluid used in these kinds of systems installed in desalination plants is steam; however, this represents a limiting element due to the low availability and location of the resource. According to this, a more suitable and achievable fluid may be used, like water or air.

Following this idea, some authors propose the use of hydroejectors to generate the required vacuum in modular MED systems, which has several advantages in its operation and manufacturing over common systems [1].

Regarding water scarcity issues in Mexico, in 2006, there were 435 installed desalination plants, being the majority of them inverse osmosis units part of commercial businesses [2]. Concerning this situation, iiDEA, an applied research group of Universidad Nacional Autónoma de México (UNAM), makes an effort to develop technologies based on the exploitation of alternative energy sources. One of its major projects is a desalination unit based on a MED system, using low-enthalpy geothermal resource as working fluid.

This system was designed with the purpose of a near-future installation in the Baja California Peninsula, Mexico, since geothermal resources and seawater are available. Fig. 2 shows a diagram of the Modular Geothermal Desalination Unit—iiDEA.

This article focuses on the analysis of the vacuum generation system, comparing the use of air and steam as driving fluid. Besides the above, the aim of this study is to determine what the system behavior would be like under certain operating conditions.

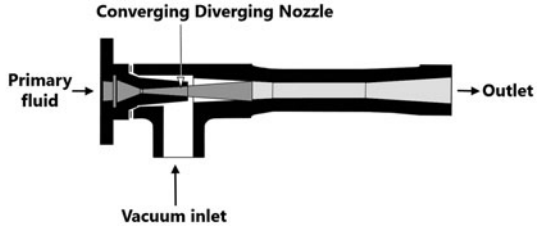

Fig. 1. Cross section of a conventional ejector.

2. Discussion

2.1. Analysis of an ejector

For this analysis, several sections of the ejector are considered, analyzing each one independently. An ejector has two inlets: the first receives the driving fluid; the second admits a fluid to be evacuated or pumped. The high-pressure, low-speed driving flow enters the ejector, coming out of the convergent–divergent nozzle at supersonic speed and working pressure, caused by the flow constriction on the throat. As a consequence of this phenomenon, the secondary flow enters the mixing chamber.

After the flows are mixed, the resulting flow goes through the diffuser, rising its pressure and lowering its speed to subsonic levels, induced by the shock wave generated inside the ejector.

For this analysis, a gas ejector modeling was taken as a starting point of the development, complementing the information with several equations of fluid mechanics and thermodynamics [3]. The following section describes the methodology applied for each of the aforementioned sections of the ejector.

2.2. Supersonic nozzle

The general configuration of a supersonic nozzle is shown in Fig. 3, where the inlet, throat, and outlet are represented by 0, t, and 1 each.

For the convergent section, an isentropic analysis is performed, since the compressibility effects are negligible. Nevertheless, in the analysis of compressible flow in the divergent section, isentropic efficiency (η_n) is considered. Isentropic efficiency takes into account the operation of the nozzle out of the design pressure range, in which shock waves may occur. Besides this, specific heat capacities are assumed constant in the analysis.

In order to obtain the main operating parameters, the calculation of density, specific heat at constant pressure (C_p), and specific heat at constant volume (C_v) (as well as the ratio of heat capacities, γ) of the driving fluid under precise stagnation conditions (T_{p0}, P_{p0}) are necessary. This section deals with the models of these parameters.

Fluid properties through an isentropic expansion can be associated with their stagnation conditions, as stated in the following equations:

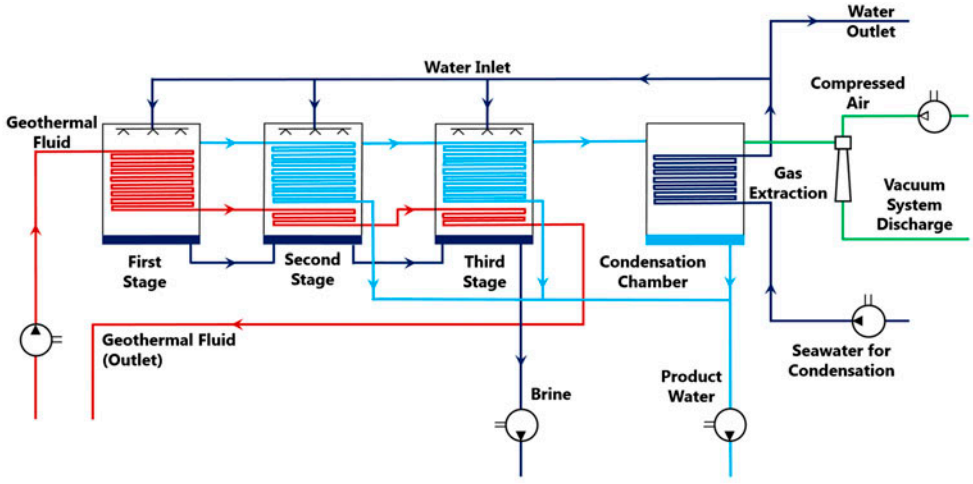

Fig. 2. Modular Geothermal Desalination Unit (MGDU—iiDEA).

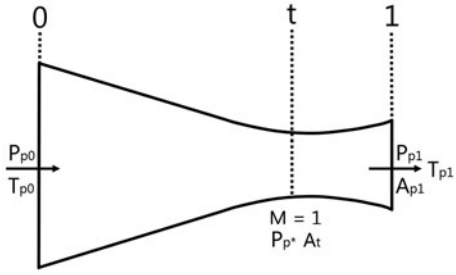

Fig. 3. Supersonic nozzle.

$$\frac{P_{p0}}{P} = \left(1 + \frac{\gamma_p - 1}{2} M^2\right)^{\frac{\gamma_p}{\gamma_p - 1}} \tag{1}$$

$$\frac{T_{p0}}{T} = 1 + \frac{\gamma_p - 1}{2} M^2 \tag{2}$$

$$\frac{\rho_{p0}}{\rho} = \left(1 + \frac{\gamma_p - 1}{2} M^2\right)^{\frac{1}{\gamma_p - 1}} \tag{3}$$

With this information, it is possible to calculate critical properties of the flow (P_*, T_*, ρ_*, V_*, and m_*). Substituting Ma = 1 into the previous equations (Eqs. (1)–(3)), Eqs. (4) through (6) are found:

$$\frac{P_*}{P_{p0}} = \left(\frac{2}{\gamma_p + 1}\right)^{\frac{\gamma_p}{\gamma_p - 1}} \tag{4}$$

$$\frac{T_*}{T_{p0}} = \frac{2}{\gamma_p + 1} \tag{5}$$

$$\frac{\rho_*}{\rho_{p0}} = \left(\frac{2}{\gamma_p + 1}\right)^{\frac{1}{\gamma_p - 1}} \tag{6}$$

On the other hand, local speed of sound in a medium with stagnation temperature T_0 is defined by:

$$c = \sqrt{\gamma_p R T_{p0}} \tag{7}$$

Eq. (7) may be rewritten using Eq. (5), such as:

$$V_* = c_* = \sqrt{\left(\frac{T_*}{T_{p0}}\right) \gamma_p R T_{p0}} \tag{8}$$

$$V_* = c_* = \sqrt{\left(\frac{2\gamma_p}{\gamma_p + 1}\right) R_p T_{p0}} \tag{9}$$

Finally, the mass flow rate at critical conditions is defined by the following equation, where it can be noticed that $A_* = A_t$:

$$m_* = \rho_* V_* A_* \tag{10}$$

Using a series of algebraic substitutions, it is possible to express Eq. (10) in terms of the stagnation properties of the fluid and its critical area. First, Eq. (9) can be rewritten as follows:

$$V_* = \sqrt{\left(\frac{2\gamma_p}{\gamma_p + 1}\right) R_p T_{p0} \left(\frac{T_*}{T_{p0}}\right)} \tag{11}$$

Inserting Eq. (5):

$$V_* = \sqrt{\left(\frac{2\gamma_p}{\gamma_p+1}\right)R_pT_{p0}\left(\frac{2}{\gamma_p+1}\right)} \tag{12}$$

$$V_* = \sqrt{\left(\frac{2}{\gamma_p+1}\right)^2\gamma_pR_pT_{p0}} \tag{13}$$

Notice that Eq. (13) may include the ratio of heat capacities:

$$V_* = \sqrt{\left(\frac{2}{\gamma_p+1}\right)^{\frac{\gamma_p+1}{\gamma_p-1}}\gamma_pR_pT_{p0}} \tag{14}$$

Then, inserting Eq. (14) into Eq. (10):

$$m_* = \rho_*A_*\sqrt{\left(\frac{2}{\gamma_p+1}\right)^{\frac{\gamma_p+1}{\gamma_p-1}}\gamma_pR_pT_{p0}} \tag{15}$$

Additionally, the Ideal gas law is stated in the following equation:

$$\rho_* = \frac{P_{p0}}{R_pT_{p0}} \tag{16}$$

Substituting Eq. (16) into Eq. (15):

$$m_* = \frac{P_{p0}}{R_pT_{p0}}A_*\sqrt{\left(\frac{2}{\gamma_p+1}\right)^{\frac{\gamma_p+1}{\gamma_p-1}}\gamma_pR_pT_{p0}} \tag{17}$$

Finally:

$$m_* = \frac{A_*P_{p0}}{\sqrt{T_{p0}}}\sqrt{\frac{\gamma_p}{R_p}\left(\frac{2}{\gamma_p+1}\right)^{\frac{\gamma_p+1}{\gamma_p-1}}} \tag{18}$$

At the inlet, the necessary pressure of the primary fluid can be calculated with the following equation, in which, Mach number is proposed ($M > 1$). Then, from Eq. (1), in relation to the inlet and outlet of que supersonic nozzle, the following equation is given:

$$P_{po} = P_{ps1}\left(1+\frac{\gamma_p-1}{2}M_{p1}^2\right)^{\frac{\gamma_p}{\gamma_p-1}} \tag{19}$$

Regarding mass conservation, the following condition must be satisfied:

$$\rho_*V_*A_* = \rho_{p1}V_{p1}A_{p1} \tag{20}$$

Substituting Eq. (18) into Eq. (20):

$$\frac{A_*P_{p0}}{\sqrt{T_{p0}}}\sqrt{\frac{\gamma_p}{R_p}\left(\frac{2}{\gamma_p+1}\right)^{\frac{\gamma_p+1}{\gamma_p-1}}} = \rho_{p1}V_{p1}A_{p1} \tag{21}$$

Therefore, substituting Eqs. (2), (3), and (7) into the above equation, it is possible to calculate the outlet area of the supersonic nozzle, shown in Eq. (22):

$$A_{p1} = \frac{A_*}{M_{p1}}\left(\frac{1+\frac{\gamma_p-1}{2}M_{p1}^2}{1+\frac{\gamma_p-1}{2}}\right)^{\frac{\gamma_p+1}{2(\gamma_p-1)}} \tag{22}$$

Finally, the diameter of the outlet is given by:

$$D_{p1s} = \sqrt{\frac{4A_{p1}}{\pi}} \tag{23}$$

Following Eqs. (2) and (3), inlet and outlet temperatures are related through the following equation:

$$T_{p1s} = \frac{T_{p0}}{1+\frac{\gamma_p-1}{2}M_{p1}^2} \tag{24}$$

The variation of density is represented by:

$$\rho_{p1s} = \frac{\rho_{p0}}{\left(1+\frac{\gamma_p-1}{2}M_{p1}^2\right)^{\frac{1}{\gamma_p-1}}} \tag{25}$$

Considering isentropic efficiency, defined as the ratio of the enthalpy of a process and the ideal enthalpy of the same process, which is known, the resulting equation is the following:

$$\eta_n = \frac{h_{p0}-h_{p1}}{h_{p0}-h_{p1i}} \tag{26}$$

The actual speed at the outlet can be calculated based on the steady flow energy equation:

$$V_{p1} = \sqrt{2\left(h_{p0}-h_{p1}\right)} \tag{27}$$

On the other hand, the relationship between real outlet temperature and stagnation temperature flow is obtained substituting Eq. (28) into Eq. (26), such as:

$$h = C_p T \tag{28}$$

$$T_{p1} = T_{po}\left[1 - \left(1 - \frac{T_{p1i}}{T_{po}}\right)\eta_n\right] \tag{29}$$

With Eqs. (2) and (29), the real pressure at the supersonic nozzle is found:

$$P_{p1} = P_{p0}\left[1 - \frac{1}{\eta_n} + \frac{1}{\eta_n\left(1 + \frac{\gamma_p - 1}{2}M_{p1}^2\right)}\right]^{\frac{\gamma_p}{\gamma_p - 1}} \tag{30}$$

Regarding mass flow rate through the nozzle, considering mass conservation, it can be expressed by Eqs. (31) and (32):

$$m_p = \rho_p A V = PAM\left(\frac{\gamma_p}{R_p T}\right)^{\frac{1}{2}} \tag{31}$$

$$\frac{A_{p1}}{A_*} = \frac{P_{p*}}{P_{p1}}\frac{1}{M_{p1}}\left(\frac{T_{p1}}{T_{p*}}\right)^{\frac{1}{2}} \tag{32}$$

Therefore, using Eqs. (29) and (30), Eq. (32), the corrected outlet area (A_{p1}) is calculated:

$$A_{p1} = \frac{A_*}{M_{p1}}\left(\frac{2}{\gamma_p - 1}\right)^{\frac{\gamma_p + 1}{2(\gamma_p - 1)}}\left[1 - \frac{1}{\eta_n} + \frac{1}{\eta_n\left(1 + \frac{\gamma_p - 1}{2}M_{p1}^2\right)}\right]^{\frac{-(\gamma_p + 1)}{2(\gamma_p - 1)}} \tag{33}$$

The real diameter is given as:

$$D_{p1} = \sqrt{\frac{4A_{p1}}{\pi}} \tag{34}$$

2.3. Analysis of the mixing zone

There are two mathematical models used for the mixing zone of an ejector. Both provide sufficient elements for the analysis of the system based on two considerations: process at constant area or at constant pressure. The first is the most used, in which, the geometrical and thermodynamic properties are crucial; the second focuses primarily on the analysis of flow behavior. Given the fact that the analysis of the ejector is part of an in-progress physical implementation of the vacuum system, only the first method will be detailed.

2.3.1. Constant area method

Fig. 4 shows the general schematic diagram for the analysis using the constant area method. The section between t and 2 demonstrates an aerodynamic throat, which strangles the secondary fluid when the Mach number reached by the primary flow is high, causing an expansion of it against the secondary flow; nevertheless, the presence of this phenomenon will be neglected, as a consequence of operating conditions of the system.

The operating conditions considered are the following:

(1) Primary and secondary flows are in steady state.
(2) Both flows are uniform in Section 1, and are completely mixed in Section 3.
(3) Both flows are considered as ideal gases.
(4) There is an adiabatic internal wall between 1 and 3.

Given the consideration of not taking the choking phenomenon of the secondary flow into account, a control volume, as shown in Fig. 5, is used.

Following the proposal of steam as secondary fluid, the necessary parameters for the calculation are the following: P_{s0}, T_{s0}, M_{s1}, and A_{m3}; with the restriction that A_{m3} must be greater than A_{p1}, as calculated before.

Starting from the given parameters P_{s0} and T_{s0}, it is possible to calculate the molar gas constant, along with the ratio of heat capacities. Therefore, knowing

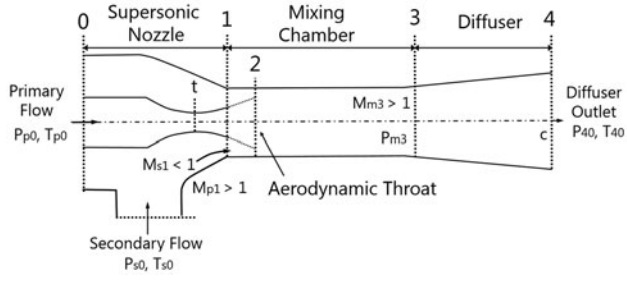

Fig. 4. Ejector with constant cross section area in mixing chamber.

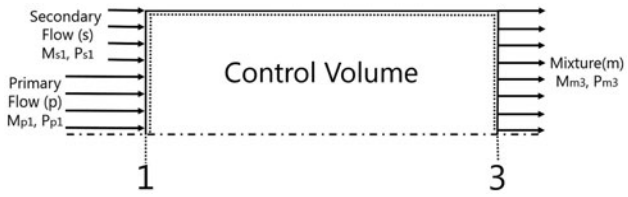

Fig. 5. Control volume used in the modeling of the constant cross section area in mixing chamber.

that $A_{s1} = A_{m3} - A_{p1}$, with the corrected value of A_{p1} and the proposed value of A_{m3}, A_{s1} may be calculated.

One of the most important factors in the ejector analysis is the drag coefficient ω, defined as the ratio of the mass of the secondary fluid inlet and the mass of the primary fluid inlet. It is possible to obtain its numerical value using the following expression:

$$\omega = \frac{P_{s0}M_{s1}}{P_{p0}M_{p1}}\sqrt{\frac{T_{p0}R_p\gamma_s}{T_{s0}R_s\gamma_p}}\left(\frac{A_{m3}}{A_*}\frac{1}{f_1\left(\gamma_p,\ M_{p1},\ \eta_n\right)} - 1\right) \times \frac{\left(1+\frac{\gamma_s-1}{2}M_{s1}^2\right)^{\frac{-(\gamma_s+1)}{2(\gamma_s-1)}}}{\left(1+\frac{\gamma_p-1}{2}M_{p1}^2\right)^{\frac{-(\gamma_p+1)}{2(\gamma_p-1)}}}\left[\left(\frac{\eta_n-1}{\eta_n}\right)\frac{\gamma_p-1}{2}M_{p1}^2+1\right]^{\frac{-\gamma_p}{\gamma_p-1}} \tag{35}$$

where function f_1 is given by the following equation:

$$f_1\left(\gamma_p,\ M_{p1},\ \eta_n\right) = \frac{1}{M_{p1}}\left(\frac{2}{\gamma_p+1}\right)^{\frac{\gamma_p+1}{2(\gamma_p-1)}} \times \left[1-\frac{1}{\eta_n}+\frac{1}{\eta_n\left(1+\frac{\gamma_p-1}{2}M_{p1}^2\right)}\right]^{\frac{-\left(\gamma_p+1\right)}{2(\gamma_p-1)}} \tag{36}$$

Thus, the mass of the secondary fluid that enters the system is:

$$m_{s1} = \omega m_{p1} \tag{37}$$

For the calculation of the inlet pressure at the mixing chamber, the following expression is used:

$$P_{s1} = P_{p1}\sqrt{\frac{T_{s0}R_s}{T_{p0}R_p}}\frac{A_{p1}}{A_{s1}}\frac{f_2(\gamma_p, M_{p1})}{f_2(\gamma_s, M_{s1})}\omega \tag{38}$$

where function f_2 is defined by the following expression:

$$f_2(\gamma,\ M) = M\left[\gamma\left(1+\frac{\gamma-1}{2}M^2\right)\right]^{\frac{1}{2}} \tag{39}$$

On the other hand, from the mass balance in Sections 1 and 3, the following is known:

$$m_{p1} + m_{s1} = m_{m3} \tag{40}$$

The following relationship is used to determine the mixture temperature at stagnation conditions:

$$T_{m0} = T_{p0}\frac{\frac{\gamma_p}{\gamma_p-1}+\frac{\gamma_s}{\gamma_s-1}\frac{R_s}{R_p}\frac{T_{s0}}{T_{p0}}\omega}{\frac{\gamma_p}{\gamma_p-1}+\frac{\gamma_s}{\gamma_s-1}\frac{R_s}{R_p}\omega} \tag{41}$$

Subsequently, the Mach number at Section 3 is calculated:

$$M_{m3} = \sqrt{\frac{-(\alpha^2-1)\pm\sqrt{(\alpha^2-2)^2+2\left(\frac{\gamma_m-1}{\gamma_m}\right)\left(\alpha^2-\frac{2\gamma_m}{\gamma_m-1}\right)}}{(\gamma_m-1)\left(\alpha^2-\frac{2\gamma_m}{\gamma_m-1}\right)}} \tag{42}$$

where α is given by the following equation:

$$\alpha = \frac{\sqrt{\frac{T_{s0}R_s}{T_{p0}R_p}}f_3(\gamma_s,\ M_{s1})\omega + f_3\left(\gamma_p,\ M_{p1}\right)}{\sqrt{\frac{T_{m0}R_m}{T_{p0}R_p}}(1+\omega)} \tag{43}$$

f_3 is given by the following equation:

$$f_3(\gamma,\ M) = \frac{1+\gamma M^2}{M}\left[\gamma\left(1+\frac{\gamma-1}{2}M^2\right)\right]^{-\frac{1}{2}} \tag{44}$$

The ratio of heat capacities of the mixture, as well as its molar gas constant is calculated using the following equations:

$$\gamma_m = \frac{\frac{\gamma_p}{\gamma_p-1}+\frac{\gamma_s}{\gamma_s-1}\frac{R_s}{R_p}\omega}{\frac{1}{\gamma_p-1}+\frac{1}{\gamma_s-1}\frac{R_s}{R_p}\omega} \tag{45}$$

$$R_m = \frac{R_p + \omega R_s}{1 + \omega} \tag{46}$$

Eq. (42) provides two results: one of them is greater than 1, while the other is less than 1. However, according to the schematic diagram used, the speed of the mixture is supersonic; therefore, the outcome of interest is the one where $M_{m3} > 1$. It should be noted that the result where $M_{m3} < 1$ is useful when a shock wave is considered in the analysis.

Finally, once the values of M_{m3} along with the other results of interest are known, pressure at Section 3 is determined:

$$P_{m3} = \frac{P_{p1}A_{p1}}{A_{m3}} \frac{1}{\left(1 + \gamma_m M_{m3}^2\right)} \times \left[\frac{P_{s1}}{P_{p1}} \frac{A_{s1}}{A_{p1}} \left(1 + \gamma_s M_{s1}^2\right) + \left(1 + \gamma_p M_{p1}^2\right)\right] \tag{47}$$

2.4. Analysis of subsonic diffuser

Using the efficiency of the diffuser, η_d (similar to the efficiency defined for the supersonic nozzle, in Eq. (26)), the ratio of inlet and outlet pressure is obtained using the following expression:

$$P_{40} = P_{m3}\left[1 + \eta_d \frac{\gamma_m - 1}{2} M_{m3}^2\right]^{\frac{\gamma_m}{\gamma_m - 1}} \tag{48}$$

Also, this section does not experience notable temperature changes; hence, it is considered constant, as long as there is not a possibility of a generation of a shock wave. In conclusion, the total compression ratio is defined by the following equation:

$$\mathrm{CR} = \frac{P_{40}}{P_{1i0}} \tag{49}$$

2.5. Calculation of the power required to drive the working fluid

Regardless of the analysis of the ejector, compressible fluids are used for this study; therefore, it is necessary to know the theoretical power required to drive the working fluid. The mathematical model used is the following:

$$\dot{W}_{\mathrm{compressor}} = \frac{mW}{\eta}\ (\mathrm{kW}) \tag{50}$$

where W is defined by:

$$W = \frac{\gamma_p}{\gamma_p - 1} P_{\mathrm{suction}} v_{\mathrm{suction}} \left[\left(\frac{P_{\mathrm{discharge}}}{P_{\mathrm{suction}}}\right)^{\frac{\gamma_p - 1}{\gamma_p}} - 1\right] \tag{51}$$

Dimensional analysis should be performed on the above equation. Specific volume (v) has units of (m^3/kg), and mass flow (m) has units of (m^3/kg). Both pressures are in (kPa). The efficiency is represented by η.

3. Results

Once the methodology for analysis of an ejector is presented, the results of the calculations are shown, taking as parameters the operational data of the iiDEA-MGD system, with a comparison between air and steam as primary fluid, and steam as secondary fluid in both cases.

For the given project planning, initial conditions of pressure and air temperature correspond to atmospheric pressure in Baja California ($P_{\mathrm{amb}} = 0.1$ MPa, $T_{\mathrm{amb}} = 30$ °C). On the other hand, the steam temperature (T_{p0}) was established based on geothermal resources of the area.

For the calculation of the supersonic nozzle, an arbitrary value of throat diameter (within a consistent range with specification sheets of commercial units with similar capabilities) was established, along with a Mach number for the desired output of the system, ensuring that the proposed Mach number was in the range set for supersonic flow, without turning into hypersonic flow.

The isentropic efficiency of the convergent, divergent, and convergent–divergent nozzles oscillate in a range between 90 and 99%; the increase or decrease in the efficiency is proportional to the size of it due to the minimization of the viscous effects when the system increases [4]. As a consequence of the above and the desired size, the following values were proposed:

$\eta_n = 90\%$, $\eta_d = 90\%$. These values ensure that the results will show the most *inefficient* performance (worst-case scenario).

The required value for the vacuum pressure in the evaporation chamber was determined from various analyses carried out by members of iiDEA. It was determined that at the outlet of the supersonic nozzle, there must be a pressure less than or equal to the pressure in the evaporation chamber in order to achieve transport of the secondary fluid.

Furthermore, according to the proposed mathematical model of the analysis of the mixing chamber, a

suitable value of $M_{s1} < 1$ was established; once the output area of the supersonic nozzle is calculated, and following the control volumes used, a value of A_{m3} greater than A_{p1} is proposed.

Finally, regarding the efficiencies of the compressors, both were set to 85% since it is a common value in these systems [5].

3.1. Analysis of the supersonic nozzle

Table 1 shows the initial known parameters of the supersonic nozzle. With the values shown in Table 1, calculated stagnation conditions of primary fluid stagnation were obtained, shown in Table 2. Furthermore, the calculated critical conditions of each flow are shown in Table 3.

Although a lower inlet pressure is required when the driving fluid is air, it is shown that the necessary mass flow is considerably greater than the required steam. Based on these values, isentropic calculations of each flow are shown in Table 4.

Considering the efficiency of the divergent section of the nozzle (η_n), a correction to the ideal parameters mentioned above is made; actual characteristics are shown in Table 5. It is shown that the correction factor significantly affects the parameters, being the outlet vacuum pressure the most disturbed element.

3.2. Analysis of the mixing chamber using a constant area method

The operating conditions of the secondary fluid are shown in Table 6. These operative conditions were the basis for the analysis, obtaining new operating parameters, shown in Table 7.

For the secondary flow, it is demonstrated that the required area to match the given conditions of speed, practically does not change in these different cases, however, the drag coefficient varies widely, being greater than 1 in both fluids, which implies that the mass flow driven is greater than the driving mass flow. As shown, the steam generates the same drag due to the steam and secondary fluid having the same nature; in addition to this, its initial enthalpy is greater.

Furthermore, as stated in the constant area mathematical model, the outlet of the control volume has supersonic speed, being air flow the fastest.

3.3. Diffuser

After analyzing the results of the mixing section, the results for the diffuser are presented. Several parameters were taken into account; among those are

Table 1
Initial known parameters

Driving fluid	Air	Steam	Units
P_{p1s}	0.009	0.009	(MPa)
M_{p1}	2.50	2.50	( )
D_*	0.010	0.010	(m)
T_{p0}	303.15	393.15	(K)
η_n	0.90	0.90	( )
η_d	0.90	0.90	( )
γ_p	1.40	1.33	( )

Table 2
Calculated stagnation conditions of primary fluid

Driving fluid	Air	Steam	Units
P_{p0}	0.154	0.157	(MPa)
ρ_{p0}	1.767	0.879	(kg/m^3)
h_{p0}	303.36	2,710.64	(kJ/kg)

Table 3
Critical conditions of each flow

Driving fluid	Air	Steam	Units
m_*	0.089	0.035	(kg/s)
A_*	0.00008	0.00008	(m^2)
P_*	0.0812	0.0845	(MPa)
T_*	252.6	337.4	(K)
ρ_*	1.12	0.55	(kg/m^3)
V_*	318.6	455.1	(m/s)

Table 4
Isentropic characteristics of driving fluid

Driving fluid	Air	Steam	Units
A_{pi1}	0.00021	0.00022	(m^2)
D_{pi1}	0.0162	0.0168	(m)
T_{pi1}	134.7	193.5	(K)
ρ_{pi1}	0.232	0.102	(kg/m^3)

Table 5
Actual characteristics of driving fluid

Driving fluid	Air	Steam	Units
A_{p1}	0.00032	0.00034	(m^2)
D_{p1}	0.02032	0.02092	(m)
T_{p1}	151.5	213.5	(K)
P_{p1}	0.00533	0.00551	(MPa)

Table 6
Initial known conditions of secondary fluid

	Secondary fluid	Units
P_{s0}	0.01	(MPa)
T_{s0}	358.15	(K)
M_{s1}	0.60	( )
A_{m3}	0.004	(m^2)

Table 7
Obtained results with constant area method

Driving fluid	Air	Steam	Units
R_s	461.52	461.52	(J/(kg K))
γ_s	1.32	1.32	( )
A_{s1}	0.00367	0.00365	(m^2)
ω	1.959	2.775	( )
m_s	0.174	0.097	(kg/s)
P_{s1}	0.00793	0.00793	(MPa)
A_{m3}	0.004	0.004	(m^2)
D_{m3}	0.0713	0.0713	(m)
m_{m3}	0.263	0.132	(kg/s)
T_{m0}	346.3	367.3	(K)
R_m	402.5	461.5	(J/(kg K))
γ_m	1.34	1.32	( )
M_{m3}	2.724	1.997	( )
P_{m3}	0.0013	0.0024	(MPa)

Table 8
Operative parameters of the diffuser

Driving fluid	Air	Steam	Units
P_{40}	0.0272	0.0156	(MPa)
CR	2.720	1.564	( )

the inlet pressure (P_{m3}) and Mach number of the flow (M_{m3}), as well as the proposed efficiency (η_d). The operative parameters for the diffuser are shown in Table 8.

While the outlet pressure of the analyzed system remains as vacuum pressure, comparing the diffuser inlet and outlet pressure, it can be noticed that the ratio of inlet and outlet pressure (P_{40}/P_{m3}) is in an acceptable range since, for all analyzed cases, it is greater than 1, reaching the greatest value when air is used as driving fluid ($P_{40}/P_{m3} = 19.89$). Based on this, it can be concluded that P_{40} is limited by operative conditions of the system, and not just the diffuser.

3.4. Required power for the system

Taking atmospheric pressure P_{amb} and flow temperature T_{p0} as suction conditions, along with stagnation conditions as discharge parameters, the necessary power to drive the working fluid to the vacuum pressure requirements is shown in Table 9.

Table 9
Required power for the system

Driving fluid	Air	Steam	Units
$\dot{W}$	5.601	4.712	(hp)

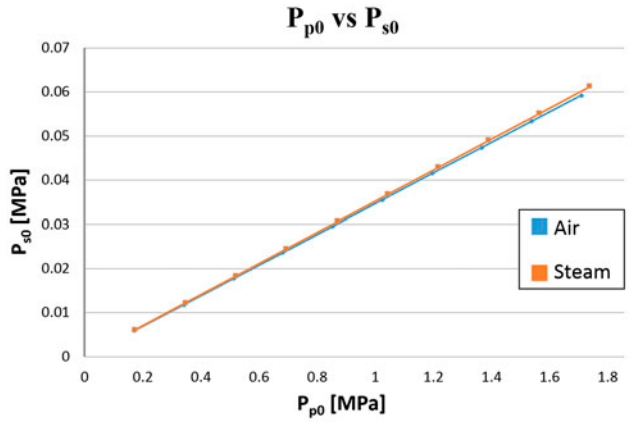

Fig. 6. Stagnation pressure of primary fluid vs. stagnation pressure of secondary fluid.

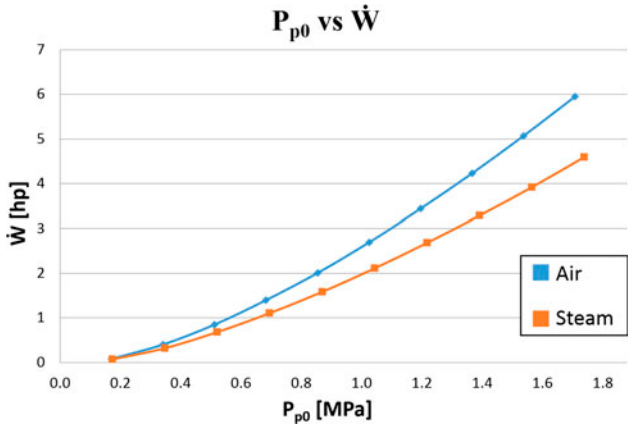

Fig. 7. Stagnation pressure of primary fluid vs. power required for the compressor.

The reported values show that the required power to drive the steam is less than the power required for air, which is considered as a decisive factor while choosing the driving flow; however, it must be taken into account the cost of installation and operation of these auxiliary systems.

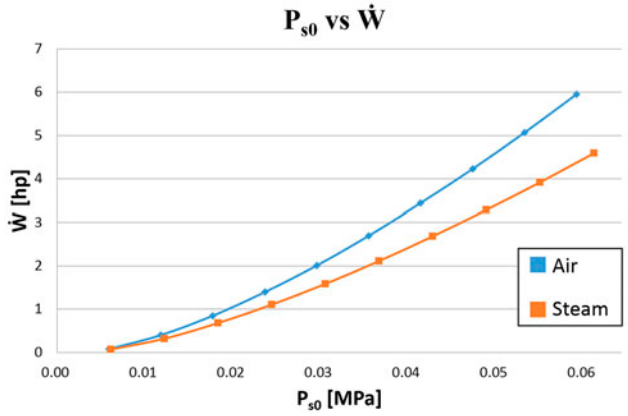

Fig. 8. Stagnation pressure of secondary fluid vs. power required for the compressor.

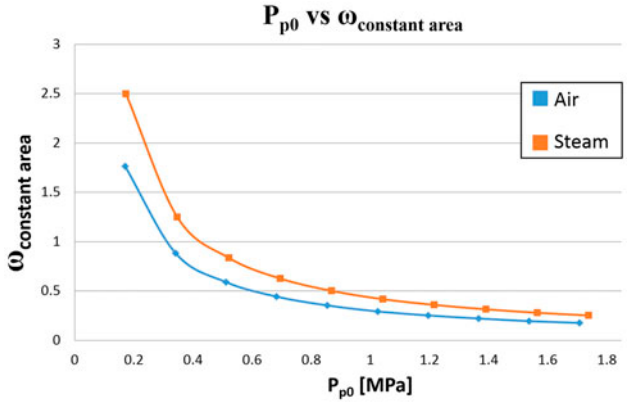

Fig. 9. Stagnation pressure of primary fluid vs. drag coefficient with constant area.

3.5. Plots

Plots with the most important parameters of the presented analysis are shown, which correspond to the vacuum pressure obtained at the inlet of the secondary flow, the required pressure of the driving fluid to generate vacuum, the required power to drive the primary flow and the drag coefficient with respect to primary fluid inlet pressure (Figs. 6–9). Note that, in order to analyze the relationships between these factors, the remaining elements, (temperature, geometry, and initial mass flow rates) must remain unaltered.

4. Conclusions

Regarding steam as driving fluid, with an initial pressure slightly greater than an air-driven ejector, the vacuum requirements of the iiDEA-MGD system are covered with a lower mass flow. This fact results in a decrease in the required power of the compressor from 5.601 to 4.712 hp. Additionally, when steam is used, the drag coefficient increases, minimizing the necessary time to induce the secondary fluid into the mixing chamber.

Still, if air is the primary fluid of the system, the above issues would not be present since it is an abundant resource in any area, without time limitations, and the only downside of its use would be the increase of the required power of the compressor.

Since the analysis presented throughout this work focuses on the implementation of a physical equipment, regardless of the fact that steam as driving flow represents the best analytical option for the ejector operation, it is necessary to evaluate parameters such as resource availability in the installation area before deciding the type of primary fluid to be used.

It is worth mentioning that the operation of the prototype MGDU—iiDEA may have fundamental limitations, specifically with regard to availability of low-enthalpy geothermal fluid and seawater; thus, if steam is used for driving the vacuum system, it is necessary to take into account that if the source is not steady, secondary equipment must be installed, such as boilers and pumps, which will add an extra cost for installation and maintenance.

Finally, it is concluded that air as working fluid is suited for laboratory tests as a consequence of its technical feasibility while steam, if available on-site, represents the best working fluid in terms of energetic feasibility.

Nomenclature

ω	—	drag coefficient
$\bar{R}$	—	universal gas constant
$\dot{W}$	—	power
A	—	area
CR	—	compression ratio
c	—	local speed of sound
c_p	—	specific heat capacity at constant pressure
c_v	—	specific heat capacity at constant volume
D	—	diameter
SD	—	solar distillation
h	—	enthalpy
iiDEA	—	Instituto de Ingeniería Desalación y Energías Alternas
iiDEA-MGDU	—	iiDEA Modular Geothermal Desalination Unit
m	—	mass flow rate
M	—	Mach number
MED	—	multiple-effect distillation
MSF	—	multi-stage flash

P	—	pressure
R	—	molar gas constant
S	—	entropy
T	—	temperature
t	—	nozzle throat
v	—	specific volume
V	—	speed
VCT	—	vapor compression by thermal means
W	—	molecular weight
γ	—	ratio of heat capacities
η	—	efficiency
ρ	—	density

Subindexes

*	—	critical conditions
0	—	stagnation conditions/supersonic nozzle inlet
1	—	supersonic nozzle exit/mixing chamber inlet
2	—	aerodynamic throat
3	—	mixing chamber outlet/diffuser inlet
4	—	diffuser outlet
amb	—	ambient
d	—	diffuser
i	—	isentropic
m	—	mixture
n	—	nozzle
p	—	primary fluid
s	—	secondary fluid

References

[1] V. Renaudin, D. Alonso, F. Kafi, J.M. Hornut, Potential application of solar heat collectors to an easymed® thermal desalination unit, in: L. Rizzuti, H.M. Ettouney, A. Cipollina, Solar Desalination for the 21st Century. Springer, Netherlands, 2007, pp. 259–270.
[2] Global Water Intelligence, IDA desalination yearbook 2006–2007, Media Analytics Ltd., Oxford, 2007.
[3] C. Liao, Gas Ejector Modeling for Design and Analysis, PhD Thesis, Texas A&M University, Texas, 2008.
[4] M.C. Potter, D.C. Wiggert, B.H. Ramadan, Mechanics of Fluids, Cengage Learning, Stamford, 2012.
[5] J.M. Campbell, Compressors, in: Gas Conditioning and Processing, Volume 2: The Equipment Modules, Campbell Petroleum Series, Oklahoma, 1992, pp. 193–238.